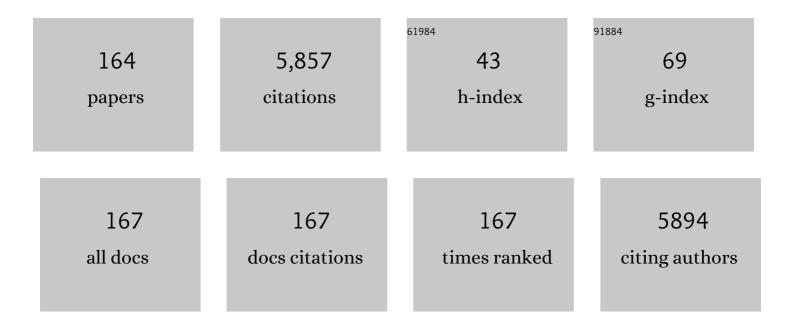
List of Publications by Year in descending order

Source: https://exaly.com/author-pdf/1632299/publications.pdf Version: 2024-02-01



#	Article	IF	CITATIONS
1	Corrosion behavior of superhydrophobic surfaces: A review. Arabian Journal of Chemistry, 2015, 8, 749-765.	4.9	421
2	An Interface Coassembly in Biliquid Phase: Toward Core–Shell Magnetic Mesoporous Silica Microspheres with Tunable Pore Size. Journal of the American Chemical Society, 2015, 137, 13282-13289.	13.7	239
3	Ultrahigh capacitive deionization performance by 3D interconnected MOF-derived nitrogen-doped carbon tubes. Chemical Engineering Journal, 2020, 390, 124493.	12.7	191
4	Electrostatic phase separation: A review. Chemical Engineering Research and Design, 2015, 96, 177-195.	5.6	181
5	Synthesis of Ordered Mesoporous Silica with Tunable Morphologies and Pore Sizes via a Nonpolar Solvent-Assisted Stöber Method. Chemistry of Materials, 2016, 28, 2356-2362.	6.7	159
6	Review of recent research on biomedical applications of electrospun polymer nanofibers for improved wound healing. Nanomedicine, 2016, 11, 715-737.	3.3	147
7	Tuning the Intermolecular Electron Transfer of Low-Dimensional and Metal-Free BCN/C ₆₀ Electrocatalysts via Interfacial Defects for Efficient Hydrogen and Oxygen Electrochemistry. Journal of the American Chemical Society, 2021, 143, 1203-1215.	13.7	140
8	Ultradispersed Palladium Nanoparticles in Three-Dimensional Dendritic Mesoporous Silica Nanospheres: Toward Active and Stable Heterogeneous Catalysts. ACS Applied Materials & Interfaces, 2015, 7, 17450-17459.	8.0	110
9	Platinum degradation mechanisms in proton exchange membrane fuel cell (PEMFC) system: A review. International Journal of Hydrogen Energy, 2021, 46, 15850-15865.	7.1	110
10	Engineering graphitic carbon nitride (g-C ₃ N ₄) for catalytic reduction of CO ₂ to fuels and chemicals: strategy and mechanism. Green Chemistry, 2021, 23, 5394-5428.	9.0	109
11	Carbon dioxide adsorption based on porous materials. RSC Advances, 2021, 11, 12658-12681.	3.6	109
12	Corrosion protection of electrospun PVDF–ZnO superhydrophobic coating. Surface and Coatings Technology, 2016, 289, 136-143.	4.8	105
13	AEO7 Surfactant as an Eco-Friendly Corrosion Inhibitor for Carbon Steel in HCl solution. Scientific Reports, 2019, 9, 2319.	3.3	91
14	Current Trends in MXene-Based Nanomaterials for Energy Storage and Conversion System: A Mini Review. Catalysts, 2020, 10, 495.	3.5	89
15	Recent advances in electroless-plated Ni-P and its composites for erosion and corrosion applications: a review. Emergent Materials, 2018, 1, 3-24.	5.7	87
16	Synthesis, characterization, and antimicrobial properties of novel double layer nanocomposite electrospun fibers for wound dressing applications. International Journal of Nanomedicine, 2017, Volume 12, 2205-2213.	6.7	85
17	Carbon/nitrogen-doped TiO2: New synthesis route, characterization and application for phenol degradation. Arabian Journal of Chemistry, 2016, 9, 229-237.	4.9	77
18	Highly efficient eco-friendly corrosion inhibitor for mild steel in 5 M HCl at elevated temperatures: experimental & molecular dynamics study. Scientific Reports, 2019, 9, 3695.	3.3	77

#	Article	IF	CITATIONS
19	Properties enhancement of Ni-P electrodeposited coatings by the incorporation of nanoscale Y2O3 particles. Applied Surface Science, 2018, 457, 956-967.	6.1	76
20	Multifunctional self-healing polymeric nanocomposite coatings for corrosion inhibition of steel. Surface and Coatings Technology, 2019, 372, 121-133.	4.8	74
21	Unveiling One-Pot Template-Free Fabrication of Exquisite Multidimensional PtNi Multicube Nanoarchitectonics for the Efficient Electrochemical Oxidation of Ethanol and Methanol with a Great Tolerance for CO. ACS Applied Materials & Interfaces, 2020, 12, 31309-31318.	8.0	73
22	The Recent Advances in the Mechanical Properties of Self-Standing Two-Dimensional MXene-Based Nanostructures: Deep Insights into the Supercapacitor. Nanomaterials, 2020, 10, 1916.	4.1	69
23	A gossypol derivative as an efficient corrosion inhibitor for St2 steel in 1ÂM HClÂ+Â1ÂM KCl: An experimental and theoretical investigation. Journal of Molecular Liquids, 2021, 328, 115475.	4.9	69
24	Fabrication of ZnO-Fe-MXene Based Nanocomposites for Efficient CO2 Reduction. Catalysts, 2020, 10, 549.	3.5	68
25	Controlling the biocorrosion of sulfate-reducing bacteria (SRB) on carbon steel using ZnO/chitosan nanocomposite as an eco-friendly biocide. Corrosion Science, 2019, 148, 397-406.	6.6	67
26	Unveiling Fabrication and Environmental Remediation of MXene-Based Nanoarchitectures in Toxic Metals Removal from Wastewater: Strategy and Mechanism. Nanomaterials, 2020, 10, 885.	4.1	64
27	Controlling the Interfacial Charge Polarization of MOF-Derived 0D–2D vdW Architectures as a Unique Strategy for Bifunctional Oxygen Electrocatalysis. ACS Applied Materials & Interfaces, 2022, 14, 3919-3929.	8.0	63
28	Unraveling template-free fabrication of carbon nitride nanorods codoped with Pt and Pd for efficient electrochemical and photoelectrochemical carbon monoxide oxidation at room temperature. Nanoscale, 2019, 11, 11755-11764.	5.6	62
29	Highly exfoliated Ti ₃ C ₂ T _{<i>x</i>} MXene nanosheets atomically doped with Cu for efficient electrochemical CO ₂ reduction: an experimental and theoretical study. Journal of Materials Chemistry A, 2022, 10, 1965-1975.	10.3	60
30	Local supersaturation and the growth of protective scales during CO2 corrosion of steel: Effect of pH and solution flow. Corrosion Science, 2017, 126, 26-36.	6.6	59
31	Rational synthesis, characterization, and application of environmentally friendly (polymer–carbon) Tj ETQq1 I Sciences Europe, 2020, 32, .	l 0.784314 5.5	rgBT /Overloo 59
32	Synthesis and electrochemical properties of nickel oxide/carbon nanofiber composites. Carbon, 2014, 71, 276-283.	10.3	58
33	Electrocoalescence of water drop trains in oil under constant and pulsatile electric fields. Chemical Engineering Research and Design, 2015, 104, 658-668.	5.6	58
34	Indentation and erosion behavior of electroless Ni-P coating on pipeline steel. Wear, 2017, 376-377, 1630-1639.	3.1	57
35	A review of MXenes as emergent materials for dye removal from wastewater. Separation and Purification Technology, 2022, 282, 120083.	7.9	56
36	Synthesis of mesoporous carbons with controlled morphology and pore diameters from SBA-15 prepared through the microwave-assisted process and their CO2 adsorption capacity. Microporous and Mesoporous Materials, 2016, 233, 44-52.	4.4	52

#	Article	IF	CITATIONS
37	Rational synthesis of one-dimensional carbon nitride-based nanofibers atomically doped with Au/Pd for efficient carbon monoxide oxidation. International Journal of Hydrogen Energy, 2019, 44, 17943-17953.	7.1	51
38	Rational Synthesis of Porous Graphitic-like Carbon Nitride Nanotubes Codoped with Au and Pd as an Efficient Catalyst for Carbon Monoxide Oxidation. Langmuir, 2019, 35, 3421-3431.	3.5	51
39	Corrosion inhibition of API X120 steel in a highly aggressive medium using stearamidopropyl dimethylamine. Journal of Molecular Liquids, 2017, 236, 220-231.	4.9	49
40	Precise fabrication of porous one-dimensional gC3N4 nanotubes doped with Pd and Cu atoms for efficient CO oxidation and CO2 reduction. Inorganic Chemistry Communication, 2019, 107, 107460.	3.9	49
41	New anti-corrosion inhibitor (3ar,6ar)-3a,6a-di-p-tolyltetrahydroimidazo[4,5-d]imidazole-2,5(1Âh,3h)-dithione for carbon steel in 1ÂM HCl medium: gravimetric, electrochemical, surface and quantum chemical analyses. Arabian Journal of Chemistry. 2020. 13. 7504-7523.	4.9	49
42	Intergranular corrosion of copper in the presence of benzotriazole. Scripta Materialia, 2006, 54, 1673-1677.	5.2	48
43	Self-Healing Performance of Multifunctional Polymeric Smart Coatings. Polymers, 2019, 11, 1519.	4.5	48
44	Electrochemical and thermodynamic study on the corrosion performance of API X120 steel in 3.5% NaCl solution. Scientific Reports, 2020, 10, 4314.	3.3	46
45	Cerium Dioxide Nanoparticles as Smart Carriers for Self-Healing Coatings. Nanomaterials, 2020, 10, 791.	4.1	45
46	Fabrication and investigation of the scratch and indentation behaviour of new generation Ni-P-nano-NiTi composite coating for oil and gas pipelines. Wear, 2019, 426-427, 265-276.	3.1	41
47	Dry ice-mediated rational synthesis of edge-carboxylated crumpled graphene nanosheets for selective and prompt hydrolysis of cellulose and eucalyptus lignocellulose under ambient reaction conditions. Green Chemistry, 2020, 22, 5437-5446.	9.0	39
48	Enhanced photocatalytic degradation of a phenolic compounds' mixture using a highly efficient TiO2/reduced graphene oxide nanocomposite. Journal of Materials Science, 2016, 51, 8331-8345.	3.7	38
49	Anti-corrosive and oil sensitive coatings based on epoxy/polyaniline/magnetite-clay composites through diazonium interfacial chemistry. Scientific Reports, 2018, 8, 13369.	3.3	37
50	Synthesis and properties of polyelectrolyte multilayered microcapsules reinforced smart coatings. Journal of Materials Science, 2019, 54, 12079-12094.	3.7	36
51	Enhanced mechanical and corrosion protection properties of pulse electrodeposited NiP-ZrO2 nanocomposite coatings. Surface and Coatings Technology, 2020, 403, 126340.	4.8	36
52	Efforts at Enhancing Bifunctional Electrocatalysis and Related Events for Rechargeable Zincâ€Air Batteries. ChemElectroChem, 2021, 8, 3998-4018.	3.4	36
53	High electrocatalytic performance of nitrogen-doped carbon nanofiber-supported nickel oxide nanocomposite for methanol oxidation in alkaline medium. Applied Surface Science, 2017, 401, 306-313.	6.1	35
54	Novel electroless deposited corrosion — resistant and anti-bacterial NiP–TiNi nanocomposite coatings. Surface and Coatings Technology, 2019, 369, 323-333.	4.8	35

#	Article	IF	CITATIONS
55	Tailored fabrication of iridium nanoparticle-sensitized titanium oxynitride nanotubes for solar-driven water splitting: experimental insights on the photocatalytic–activity–defects relationship. Catalysis Science and Technology, 2020, 10, 801-809.	4.1	33
56	Analysis of partial electrocoalescence by Level-Set and finite element methods. Chemical Engineering Research and Design, 2016, 114, 180-189.	5.6	32
57	Effect of load, temperature and humidity on the pH of the water drained out from H2/air polymer electrolyte membrane fuel cells. Journal of Power Sources, 2009, 190, 264-270.	7.8	31
58	Recent advances in corrosion resistant superhydrophobic coatings. Corrosion Reviews, 2018, 36, 127-153.	2.0	31
59	New Electrospun Polystyrene/Al2O3 Nanocomposite Superhydrophobic Coatings; Synthesis, Characterization, and Application. Coatings, 2018, 8, 65.	2.6	31
60	Effect of electroless bath composition on the mechanical, chemical, and electrochemical properties of new NiP–C3N4 nanocomposite coatings. Surface and Coatings Technology, 2019, 362, 239-251.	4.8	31
61	An efficient green ionic liquid for the corrosion inhibition of reinforcement steel in neutral and alkaline highly saline simulated concrete pore solutions. Scientific Reports, 2020, 10, 14565.	3.3	31
62	Facile one-step aqueous-phase synthesis of porous PtBi nanosponges for efficient electrochemical methanol oxidation with a high CO tolerance. Journal of Electroanalytical Chemistry, 2022, 916, 116361.	3.8	30
63	Synthesis and characterisation of Ni–B/Ni–P–CeO2 duplex composite coatings. Journal of Applied Electrochemistry, 2018, 48, 391-404.	2.9	29
64	Corrosion Inhibition of Mild Steel in Sulfuric Acid by a Newly Synthesized Schiff Base: An Electrochemical, DFT, and Monte Carlo Simulation Study. Electroanalysis, 2020, 32, 3145-3158.	2.9	29
65	Porous high-entropy alloys as efficient electrocatalysts for water-splitting reactions. Electrochemistry Communications, 2022, 136, 107207.	4.7	29
66	Kinetics of the electrochemical deposition of sulfur from sulfide polluted brines. Journal of Applied Electrochemistry, 2007, 37, 395-404.	2.9	28
67	Indentation and bending behavior of electroless Ni-P-Ti composite coatings on pipeline steel. Surface and Coatings Technology, 2018, 334, 243-252.	4.8	28
68	Synthesis, Characterization, and Application of Novel Ni-P-Carbon Nitride Nanocomposites. Coatings, 2018, 8, 37.	2.6	28
69	Engineering of Pt-based nanostructures for efficient dry (CO2) reforming: Strategy and mechanism for rich-hydrogen production. International Journal of Hydrogen Energy, 2022, 47, 5901-5928.	7.1	28
70	Rational synthesis of three-dimensional core–double shell upconversion nanodendrites with ultrabright luminescence for bioimaging application. Chemical Science, 2019, 10, 7591-7599.	7.4	27
71	Unveiling one-pot scalable fabrication of reusable carboxylated heterogeneous carbon-based catalysts from eucalyptus plant with the assistance of dry ice for selective hydrolysis of eucalyptus biomass. Renewable Energy, 2020, 153, 998-1004.	8.9	27
72	Improved self-healing performance of polymeric nanocomposites reinforced with talc nanoparticles (TNPs) and urea-formaldehyde microcapsules (UFMCs). Arabian Journal of Chemistry, 2021, 14, 102926.	4.9	27

#	Article	IF	CITATIONS
73	Electrospun highly corrosion-resistant polystyrene–nickel oxide superhydrophobic nanocomposite coating. Journal of Applied Electrochemistry, 2021, 51, 1605-1618.	2.9	26
74	Investigation of fracture behavior of annealed electroless Ni-P coating on pipeline steel using acoustic emission methodology. Surface and Coatings Technology, 2017, 326, 336-342.	4.8	25
75	Effect of sulfide pollution on the stability of the protective film of benzotriazole on copper. Applied Surface Science, 2007, 253, 8986-8991.	6.1	24
76	Highly Ordered Nanoporous Carbon Films with Tunable Pore Diameters and their Excellent Sensing Properties. Chemistry - A European Journal, 2015, 21, 697-703.	3.3	24
77	Synthesis and Characterization of Scratch-Resistant Ni-P-Ti-Based Composite Coating. Tribology Transactions, 2019, 62, 880-896.	2.0	24
78	Enhancing the corrosion resistance of reinforcing steel under aggressive operational conditions using behentrimonium chloride. Scientific Reports, 2019, 9, 18115.	3.3	24
79	Corrosion and Heat Treatment Study of Electroless NiP-Ti Nanocomposite Coatings Deposited on HSLA Steel. Nanomaterials, 2020, 10, 1932.	4.1	24
80	Titanium Carbide (Ti ₃ C ₂ T _x) MXene Ornamented with Palladium Nanoparticles for Electrochemical CO Oxidation. Electroanalysis, 2022, 34, 677-683.	2.9	24
81	Temperature gradients measurements within a segmented H2/air PEM fuel cell. Journal of Power Sources, 2007, 172, 209-214.	7.8	23
82	Ecotoxicological Assessment of Thermally- and Hydrogen-Reduced Graphene Oxide/TiO2 Photocatalytic Nanocomposites Using the Zebrafish Embryo Model. Nanomaterials, 2019, 9, 488.	4.1	23
83	Calix[4]arene-clicked clay through thiol-yne addition for the molecular recognition and removal of Cd(II) from wastewater. Separation and Purification Technology, 2020, 251, 117383.	7.9	22
84	Multilevel Self-Healing Characteristics of Smart Polymeric Composite Coatings. ACS Applied Materials & Interfaces, 2021, 13, 51459-51473.	8.0	22
85	Effect of Temperature on the Corrosion Behavior of API X120 Pipeline Steel in H2S Environment. Journal of Materials Engineering and Performance, 2017, 26, 3775-3783.	2.5	21
86	Tailoring the defects of sub-100 nm multipodal titanium nitride/oxynitride nanotubes for efficient water splitting performance. Nanoscale Advances, 2021, 3, 5016-5026.	4.6	21
87	The Role of Oxygen on the Stability of Crevice Corrosion. Journal of the Electrochemical Society, 2002, 149, B198.	2.9	19
88	Data on the catalytic CO oxidation and CO2 reduction durability on gC3N4 nanotubes Co-doped atomically with Pd and Cu. Data in Brief, 2019, 26, 104495.	1.0	19
89	Nitrogenization of Biomass-Derived Porous Carbon Microtubes Promotes Capacitive Deionization Performance. Bulletin of the Chemical Society of Japan, 2021, 94, 1645-1650.	3.2	19
90	Effect of the graphene oxide reduction method on the photocatalytic and electrocatalytic activities of reduced graphene oxide/TiO ₂ composite. RSC Advances, 2015, 5, 71988-71998.	3.6	18

#	Article	IF	CITATIONS
91	An efficient eco advanced oxidation process for phenol mineralization using a 2D/3D nanocomposite photocatalyst and visible light irradiations. Scientific Reports, 2017, 7, 9898.	3.3	17
92	Designing and performance evaluation of polyelectrolyte multilayered composite smart coatings. Progress in Organic Coatings, 2019, 137, 105319.	3.9	17
93	The localized corrosion of Al 6XXX alloys. Jom, 2001, 53, 42-46.	1.9	16
94	Kinetics of corrosion inhibition of benzotriazole to copper in 3.5% NaCl. Materials and Corrosion - Werkstoffe Und Korrosion, 2008, 59, 691-696.	1.5	16
95	Photocatalysis of TiO2 - Supported Graphene Oxide and its Reduced Form towards Phenol Degradation. ECS Transactions, 2015, 64, 1-12.	0.5	16
96	Linear dynamics modelling of droplet deformation in a pulsatile electric field. Chemical Engineering Research and Design, 2016, 114, 162-170.	5.6	16
97	The Effects of Cr/Mo Micro-Alloying on the Corrosion Behavior of Carbon Steel in CO ₂ -Saturated (Sweet) Brine under Hydrodynamic Control. Journal of the Electrochemical Society, 2018, 165, C278-C288.	2.9	16
98	A review of bipolar plates materials and graphene coating degradation mechanism in proton exchange membrane fuel cell. International Journal of Energy Research, 2022, 46, 3766-3781.	4.5	16
99	Porous ternary Pt-based branched nanostructures for electrocatalytic oxygen reduction. Electrochemistry Communications, 2022, 136, 107237.	4.7	15
100	Organ-specific toxicity evaluation of stearamidopropyl dimethylamine (SAPDMA) surfactant using zebrafish embryos. Science of the Total Environment, 2020, 741, 140450.	8.0	14
101	Self-Healing Performance of Smart Polymeric Coatings Modified with Tung Oil and Linalyl Acetate. Polymers, 2021, 13, 1609.	4.5	14
102	Synergistic Effect of O ₃ and H ₂ O ₂ on the Visible Photocatalytic Degradation of Phenolic Compounds Using TiO ₂ /Reduced Graphene Oxide Nanocomposite. Science of Advanced Materials, 2017, 9, 739-746.	0.7	14
103	Erosion Behavior of API X120 Steel: Effect of Particle Speed and Impact Angle. Coatings, 2018, 8, 343.	2.6	13
104	Smart design of exquisite multidimensional multilayered sand-clock-like upconversion nanostructures with ultrabright luminescence as efficient luminescence probes for bioimaging application. Mikrochimica Acta, 2020, 187, 527.	5.0	12
105	Development of spin-coated Si/TiOx/Pt/TiOx electrodes for the electrochemical ozone production. Applied Surface Science, 2009, 255, 8458-8463.	6.1	11
106	Temperature effect on the recovery of SO2-Poisoned GC/Nano-Pt electrode towards oxygen reduction. Journal of Solid State Electrochemistry, 2010, 14, 1727-1734.	2.5	11
107	Hydrothermal-induced growth of Ca10V6O25 crystals with various morphologies in a strong basic medium at different temperatures. Materials Research Bulletin, 2013, 48, 1388-1396.	5.2	11
108	High Electrocatalytic Performance of CuCoNi@CNTs Modified Glassy Carbon Electrode towards Methanol Oxidation in Alkaline Medium. Applied Sciences (Switzerland), 2017, 7, 64.	2.5	11

#	Article	IF	CITATIONS
109	Chitosan/Lignosulfonate Nanospheres as "Green―Biocide for Controlling the Microbiologically Influenced Corrosion of Carbon Steel. Materials, 2020, 13, 2484.	2.9	11
110	Superior Corrosion and UV-Resistant Highly Porous Poly(vinylidene) Tj ETQq0 0 0 rgBT /Overlock 10 Tf 50 707 Materials, 2022, 4, 1358-1367.	Td (fluoride 4.4	e- <i>co</i> -he> 11
111	Effects of microstructures on hydrogen induced cracking of electrochemically hydrogenated double notched tensile sample of 4340 steel. Materials Science & Engineering A: Structural Materials: Properties, Microstructure and Processing, 2016, 659, 242-255.	5.6	10
112	Simulation studies of Sn-based perovskites with Cu back-contact for non-toxic and non-corrosive devices. Journal of Materials Research, 2019, 34, 2789-2795.	2.6	10
113	Design of hybrid clay/ polypyrrole decorated with silver and zinc oxide nanoparticles for anticorrosive and antibacterial applications. Progress in Organic Coatings, 2020, 149, 105918.	3.9	10
114	Microbiologically-influenced corrosion of the electroless-deposited NiP-TiNi – Coating. Arabian Journal of Chemistry, 2021, 14, 103445.	4.9	10
115	Superhydrophobic and Corrosion Behavior of Electrospun PVDF-ZnO Coating. ECS Transactions, 2015, 64, 57-67.	0.5	9
116	Effect of Cr/Mo on the Protectiveness of Corrosion Scales on Carbon Steel in Sweet Medium under High Flow Regime. ECS Transactions, 2017, 80, 509-517.	0.5	9
117	Effects of Oxygen on Scale Formation in CO ₂ Corrosion of Steel in Hot Brine: In Situ Synchrotron X-ray Diffraction Study of Anodic Products. Journal of the Electrochemical Society, 2018, 165, C756-C761.	2.9	9
118	Data on structural and composition-related merits of gC3N4 nanofibres doped and undoped with Au/Pd at the atomic level for efficient catalytic CO oxidation. Data in Brief, 2019, 27, 104734.	1.0	9
119	Novel Enzyme-Free Multifunctional Bentonite/Polypyrrole/Silver Nanocomposite Sensor for Hydrogen Peroxide Detection over a Wide pH Range. Sensors, 2019, 19, 4442.	3.8	9
120	Spectral, thermal, antimicrobial studies for silver(I) complexes of pyrazolone derivatives. BMC Chemistry, 2020, 14, 69.	3.8	8
121	Data on the synthesis and characterizations of carboxylated carbon-based catalyst from eucalyptus as efficient and reusable catalysts for hydrolysis of eucalyptus. Data in Brief, 2020, 30, 105520.	1.0	8
122	AEO-7 surfactant is "super toxic―and induces severe cardiac, liver and locomotion damage in zebrafish embryos. Environmental Sciences Europe, 2020, 32, .	5.5	8
123	Superior Electrocatalysis of Spin-coated Titanium Oxide Electrodes for the Electrochemical Ozone Production. Chemistry Letters, 2007, 36, 1046-1047.	1.3	7
124	A quartz crystal microbalance study of the kinetics of interaction of benzotriazole with copper. Journal of Applied Electrochemistry, 2007, 37, 1177-1182.	2.9	7
125	The missing piece of the puzzle regarding the relation between the degree of superhydrophobicity and the corrosion resistance of superhydrophobic coatings. Electrochemistry Communications, 2018, 91, 41-44.	4.7	7
126	An Extraordinary Effect of Benzotriazole and Sulfide Ions on the Corrosion of Copper. Electrochemical and Solid-State Letters, 2006, 9, B19.	2.2	6

#	Article	IF	CITATIONS
127	Graphene /TiO2 Composite Electrode: Synthesis and Application towards the Oxygen Reduction Reaction. ECS Transactions, 2014, 61, 13-26.	0.5	6
128	Effect of Trace H ₂ S on the Scale Formation Behavior in a Predominant CO ₂ Environment under Hydrodynamic Control: Role of Cr/Mo Micro-Alloying in Plain Carbon Steel. Journal of the Electrochemical Society, 2019, 166, C3233-C3240.	2.9	6
129	Controlled synthesis of carbon nitride-TiO2 nanocomposites for prompt photocatalytic degradation of individual and mixed organic dyes at room temperature. Emergent Materials, 2020, 3, 955-963.	5.7	6
130	A simple in situ characterization technique for the onset of the chemical degradation of PEM fuel cells' fluorinated membranes. Electrochemistry Communications, 2008, 10, 1732-1735.	4.7	5
131	A Smart Colorimetric Platform for Detection of Methanol, Ethanol and Formic Acid. Sensors, 2022, 22, 618.	3.8	5
132	Rational Synthesis of Mixed Metal Oxide Clusters Supported on a Partially Etched MAX Phase for Efficient Electrocatalytic CO2 Conversion. Topics in Catalysis, 0, , 1.	2.8	5
133	Effect of Operating Conditions on the Acidity of H2/Air PEM Fuel Cells' Water. ECS Transactions, 2009, 16, 543-550.	0.5	4
134	Effects of superelastic nano-NiTi additions on electroless Ni –P coating properties under bending. Surface and Coatings Technology, 2019, 378, 125064.	4.8	4
135	Eco-friendly highly efficient BN/rGO/TiO2 nanocomposite visible-light photocatalyst for phenol mineralization. Environmental Science and Pollution Research, 2021, 28, 62771-62781.	5.3	4
136	Impact of Prolonged Exposure to Sour Service on the Mechanical Properties and Corrosion Mechanism of NACE Carbon Steel Material Used in Wet Sour Gas Multiphase Pipeline. Sustainability, 2022, 14, 8015.	3.2	4
137	Toward an Accurate Spectrophotometric Evaluation of the Efficiencies of Photocatalysts in Processes Involving Their Separation Using Nylon Membranes. Catalysts, 2018, 8, 576.	3.5	3
138	Investigation of the Mechanical Behavior of Electroless Ni–P–Ti Composite Coatings. Journal of Engineering Materials and Technology, Transactions of the ASME, 2020, 142, .	1.4	3
139	A Hybrid Photo-Electro Catalytic Conversion of Carbon dioxide Using CuO–MgO Nanocomposite. Topics in Catalysis, 0, , 1.	2.8	3
140	Surface Layer Formation in the Earliest Stages of Corrosion of Steel in CO ₂ -Saturated Brine at 80°C: Studied by In Situ Synchrotron X-ray Methods. Journal of the Electrochemical Society, 2018, 165, C842-C847.	2.9	2
141	Data on the fabrication of hybrid calix [4]arene-modified natural bentonite clay for efficient selective removal of toxic metals from wastewater at room temperature. Data in Brief, 2021, 35, 106799.	1.0	2
142	Caprylamidopropyl Betaine as a highly efficient eco-friendly corrosion inhibitor for API X120 steel in 1 M H2SO4. Egyptian Journal of Chemistry, 2019, .	0.2	2
143	Efforts at Enhancing Bifunctional Electrocatalysis and Related Events for Rechargeable Zincâ€Air Batteries. ChemElectroChem, 2021, 8, 3996-3996.	3.4	2
144	Nickel Oxide Carbon Nanofiber Composite for Electrochemical Oxidation of Methanol. ECS Transactions, 2014, 61, 1-11.	0.5	1

#	Article	IF	CITATIONS
145	Formation and Structure of Sulfide Deposits on Carbon Steel Under Free Corrosion Potential. Corrosion, 2021, 77, 1164-1177.	1.1	1
146	Corrosion behavior of high strength low alloy HSLA steel in 35 wt% NaCl solution containing diethylenetriamine DETA as corrosion inhibitor. , 2018, , .		1
147	Atmospheric Corrosion of 904L Austenitic Stainless Steel at Different Environments. ECS Meeting Abstracts, 2017, , .	0.0	1
148	Template-assisted growth of rhodium nanowire contacts to silicon nanowires. International Journal of Nanomanufacturing, 2009, 4, 146.	0.3	0
149	Effect of Relative Humidity on Temperature and Current Distributions within a Segmented H2/Air PEM Fuel Cell. ECS Transactions, 2011, 35, 293-302.	0.5	Ο
150	Corrosion Inhibition of C-Steel Using Supported and Non-Supported Cu-Nanoparticles/Benzotriazole. ECS Transactions, 2014, 61, 15-23.	0.5	0
151	Synthesis and Optimization of a Highly Stable and Efficient BN/TiO 2 Nanocomposite for Phenol Degradation: A Photocatalytic, Mechanistic and Environmental Impact Study. ChemistrySelect, 2021, 6, 5752-5762.	1.5	0
152	Effect of Cr/Mo on the Protectiveness of Corrosion Scales on Carbon Steel in Sweet Medium Under Hydrodynamic Condition. ECS Meeting Abstracts, 2017, , .	0.0	0
153	1st Cut Spent Pot Liner-Modified Epoxy Coatings for C-Steel. ECS Meeting Abstracts, 2017, , .	0.0	0
154	Carbon Nitride/TiO2 Nanocomposite in Treatment of Water Contaminated with Phenol. ECS Meeting Abstracts, 2017, , .	0.0	0
155	Artificial Pits for the Study of Underdeposit Corrosion Kinetics. ECS Meeting Abstracts, 2017, , .	0.0	0
156	Sulfide Scaling and Corrosion of Carbon Steel in a Sour Medium. ECS Meeting Abstracts, 2017, , .	0.0	0
157	The Interdependent Deposit-Steel Interaction during Underdeposit Corrosion (UDC). ECS Meeting Abstracts, 2018, , .	0.0	0
158	Under-Deposit Corrosion (UDC): The Hidden Cause of Major Asset Failures in the Oil and Gas Industry. ECS Meeting Abstracts, 2018, , .	0.0	0
159	Understanding the Scales Formation Inhibition Mechanism on C-Steel in a Sour media. ECS Meeting Abstracts, 2018, , .	0.0	0
160	Understanding the Scales Formation Inhibition Mechanism on C-Steel in a Sour Media. ECS Meeting Abstracts, 2019, , .	0.0	0
161	Highly UV and Corrosion - Resistant Poly(vinylidene fluoride)â€Coâ€Hexafluoropropylene - Carbon Nanotubes Superhydrophobic Nanocomposite Coating for C-Steel. ECS Meeting Abstracts, 2019, , .	0.0	0
162	The Interdependent Deposit-Metal Interaction during Underdeposit Corrosion (UDC). ECS Meeting Abstracts, 2019, , .	0.0	0

#	Article	IF	CITATIONS
163	Study of In Vitro Biodegradation Behavior of Mg–2.5Zn–xES Composite. Minerals, Metals and Materials Series, 2020, , 253-258.	0.4	0
164	New Highly Microbial-Induced Corrosion-Resistant Ni-P-Based Coating with Superior Mechanical Properties ECS Meeting Abstracts, 2020, MA2020-02, 3821-3821.	0.0	0